RAPID COMMUNICATIONS

PHYSICAL REVIEW C VOLUME 51, NUMBER 3 MARCH 1995

Measurement of the reaction $^{12}C(\nu_\mu,\mu^-)X$ near threshold

M. Albert,[12] C. Athanassopoulos,[13] L. B. Auerbach,[13] D. Bauer,[3] R. Bolton,[7] B. Boyd,[9] R. L. Burman,[7] I. Cohen,[6] D. O. Caldwell,[3] B. D. Dieterle,[10] J. B. Donahue,[7] A. M. Eisner,[4] A. Fazely,[11] F. J. Federspiel,[7] G. T. Garvey,[7] R. M. Gunasingha,[8] V. Highland,[13,*] J. Hill,[12] R. Imlay,[8] K. Johnston,[9] W. C. Louis,[7] A. Lu,[3] A. K. Mann,[12] J. Margulies,[13] K. McIlhany,[1] W. Metcalf,[8] R. A. Reeder,[10] V. Sandberg,[7] M. Schillaci,[7] D. Smith,[5] I. Stancu,[1] W. Strossman,[1] M. K. Sullivan,[4] G. J. VanDalen,[1] W. Vernon,[2,4] Y-X. Wang,[4] D. H. White,[7] D. Whitehouse,[7] D. Works,[13] Y. Xiao,[13] and S. Yellin[3]

[1]*University of California, Riverside, California 92521*

[2]*University of California, San Diego, California 92093*

[3]*University of California, Santa Barbara, California 93106*

[4]*University of California Intercampus Institute for Research at Particle Accelerators, Stanford, California 94309*

[5]*Embry Riddle Aeronautical University, Prescott, Arizona 86301*

[6]*Linfield College, McMinnville, Oregon 97128*

[7]*Los Alamos National Laboratory, MS H846, Los Alamos, New Mexico 87545*

[8]*Louisiana State University, Baton Rouge, Louisiana 70803*

[9]*Louisiana Tech University, Ruston, Louisiana 71272*

[10]*University of New Mexico, Albuquerque, New Mexico 87131*

[11]*Southern University, Baton Rouge, Louisiana 70813*

[12]*University of Pennsylvania, Philadelphia, Pennsylvania 19104*

[13]*Temple University, Philadelphia, Pennsylvania 19122*

(Received 28 September 1994)

The reaction $^{12}C(\nu_\mu,\mu^-)X$ has been measured near threshold using a π^+ decay-in-flight ν_μ beam from the Los Alamos Meson Physics Facility and a massive liquid scintillator neutrino detector (LSND). In the energy region $123.7<E_\nu<280$ MeV, the measured spectral shape is consistent with that expected from the Fermi-gas model (FGM). However, the measured flux-averaged inclusive cross section $\{[8.3\pm0.7(\text{stat})\pm1.6(\text{syst})]\times10^{-40}\ \text{cm}^2\}$ is more than a factor of 2 lower than that predicted by the Fermi-gas model and by a recent random phase approximation calculation.

PACS number(s): 25.30.Pt

There has been little information to date on low-energy neutrino-nucleus scattering despite its potential application to nuclear structure studies. This process principally involves axial-vector nuclear currents and consequently provides different information than low-energy electron-nucleus scattering, which is sensitive only to polar-vector currents. While the coupling of the $W^\pm$ to a free nucleon is well understood at low Q^2 ($Q^2<1$ GeV^2), calculation of the $(\nu,l^\pm)$ inclusive cross section from a nucleus is beyond the capabilities of present models. The Fermi-gas model (FGM) [1] is not expected to reliably predict the cross section in cases where the momentum transferred to the target is less than twice the average Fermi momentum of the bound nucleons in the target. For the inclusive yield of $^{12}C(\nu_\mu,\mu^-)X$ near threshold, the momentum transfer is below the above requirement; hence the FGM can provide only qualitative guidance. An improved description can be obtained using a model that includes the residual particle-hole interaction via the random-phase approximation (RPA). How well this particular model will work in a specific case is a matter for experiment to decide. However, it does not appear that this problem is beyond the scope of present day nuclear theory if more complete dynamical descriptions are employed. It should be noted that these inclusive charged-current processes, $A(\nu,l^\pm)X$, have taken on new importance in recent years as they are central to the detection process in several neutrino detectors [2].

We report here measurements of the salient features of the reaction $^{12}C(\nu_\mu,\mu^-)X$ from threshold (123.7 MeV) to 280 MeV neutrino energy. The data were obtained in the initial run of the liquid scintillator neutrino detector (LSND) at the Los Alamos Meson Physics Facility (LAMPF).

LSND is a cylindrical imaging Čerenkov detector 8.3 m long and 5.7 m in diameter with its axis horizontal. It consists of 197 m^3 of mineral oil viewed by 1220 20-cm-diam photomultiplier tubes (PMTs), which cover 24.8% of the detector's inner surface. A small amount of scintillator (0.031 g/l butyl-PBD) is dissolved in the mineral oil, so that both the scintillation and Čerenkov light produced by charged particles may be observed and resolved [3]. For a given amount of detected light, the ratio of light in the Čerenkov cone to isotropic light (which includes wave-shifted Čerenkov light) facilitates identification of particle type. For highly relativistic particles, this ratio is approximately 1:4. The spatial origin of the light associated with an event can be localized to within 25 cm rms using the photon arrival times at each hit PMT. For electrons, the relationship between the total detected PMT charge and particle energy is determined by the 52.8 MeV end point of electrons from the decay of stopping cosmic ray muons (the Michel spectrum). In this spectrum, 32 PEs per MeV are detected, where a PE is defined as the

*Deceased.

peak of the PMT response to a single photoelectron. The energy resolution at the end point of the spectrum is 7%. The corresponding relationship between charge and energy for other particle types is determined by a GEANT-based Monte Carlo simulation of LSND [4] which reproduces the observed Michel spectrum and incorporates data from an exposure of a sample of LSND scintillator to protons and electrons of known energy [3].

The midpoint of the LSND detector is located 29 m downstream of the LAMPF A-6 proton beam dump at 12° from the axis of the proton beam. LSND is surrounded (except for the bottom) by a highly efficient cosmic ray veto counter [5], which is crucial for eliminating backgrounds that would otherwise arise from the 4 kHz rate of cosmic muons in the detector.

The trigger requires signals above threshold in at least 100 of the detector PMTs, and fewer than 6 hit tubes in the veto counter. When this trigger is satisfied, the event is read out along with every other event that fired either the veto counter or at least 18 PMTs in the detector within the previous 51.2 μs. To remove the burden on the data acquisition system of recording decay electrons from stopping cosmic muons, the trigger is disabled for 7 muon lifetimes following each firing of the veto.

For the data reported here, a 780 MeV proton beam at 600–700 μA was delivered at a 7.1% duty factor to the A-6 proton beam dump. The integrated intensity was 1625 C. The beam dump configuration consisted of a 20 cm long water target, several inserts used for isotope production, and a copper proton beam stop. The water target serves as the main source of pions for both the decay-in-flight (DIF) and decay-at-rest (DAR) neutrino beams, with a smaller contribution to the DAR neutrinos arising from the beam stop directly. Because of the 123.7 MeV threshold for the $^{12}C(\nu_\mu,\mu^-)X$ reaction, only DIF neutrinos contribute.

The DIF neutrino flux is calculated by a Monte Carlo simulation of the beam dump [6], and includes the flux from the two thin targets well upstream of the beam dump, whose contributions are significant only at the highest neutrino energies. Because the decay chain $\pi^+ \rightarrow \mu^+ + \nu_\mu$ followed by $\mu^+ \rightarrow e^+ + \nu_e + \bar{\nu}_\mu$ is dominant, the integrated neutrino flux from π^+ DIF is constrained by measurements of the neutrino flux from μ^+ DAR. The Monte-Carlo-calculated flux from DAR has been verified in an independent measurement [7] to an accuracy of $\pm 8\%$ and confirmed in an experiment that measured ν_e elastic scattering from electrons [8] to an accuracy of $\pm 15\%(\text{stat}) \pm 9\%(\text{syst})$. The shape of the DIF neutrino spectrum is determined mostly from geometrical factors and only to some smaller degree by the pion production data. Because of this, the point-to-point uncertainties in the calculated spectrum are small compared to the uncertainty in the overall normalization. We estimate that these two effects together give rise to a 15% uncertainty in the flux-averaged cross section. The DIF neutrino flux distribution is shown in Fig. 1.

The quasielastic process $^{12}C(\nu_\mu,\mu^-)X$ produces a muon in the interior of the detector, usually accompanied by a promptly ejected proton. The muon + proton signal is followed by an electron from the ($\tau = 2.03$ μs) decay of that muon in mineral oil [9]. Thus we select pairs of events occurring within 17 μs of each other and reconstructing within

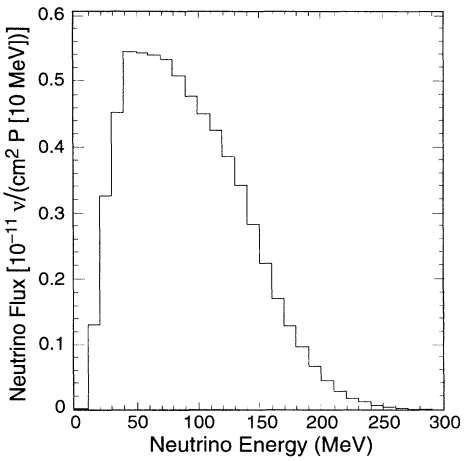

FIG. 1. The calculated energy spectrum of muon neutrinos from the decay-in-flight beam.

200 cm of each other. Requiring less than 4 hit tubes in the veto counter suppresses the cosmic ray muon contribution by a factor of 5×10^{-5}. The majority of the remaining cosmic-ray-induced events are eliminated by imposing the following additional criteria: First, the number of PEs detected for the first event (the $\mu^- + p$ candidate) is required to be less than the maximum expected from a $C(\nu_\mu,\mu^-)X$ event, given the flux shown in Fig. 1. Second, the energy associated with the electron candidate is required to be less than 60 MeV, and above the end point energy (13.6 MeV) of ^{12}B beta decay. (^{12}B is formed in the detector by the capture of cosmic ray μ^- on ^{12}C. This cut is accomplished by requiring the electron to fire more than 250 PMTs.) Finally, both events are required to have reconstructed positions within the central 108 m^3 fiducial volume. The efficiency of these selection criteria is $34 \pm 4\%$ (see Table I). Because of greater background for the lowest energy muons, tighter selection criteria (listed in Table I) were applied to these events, reducing the efficiency for those muons to $25 \pm 3\%$. (Less than 10% of the

TABLE I. The efficiencies for selection of quasielastic events. As seen in Fig. 2, the efficiencies for the spatial and temporal coincidences are essentially 100%.

Source	Efficiency
veto counter inactive	0.77 ± 0.02
computer ready	0.97 ± 0.01
μ^- not captured	0.92 ± 0.01
μ^- lives longer than 0.7 μs	0.71 ± 0.04
μ^- and e^- in fiducial volume	0.78 ± 0.08
e^- fires more than 250 PMTs	0.90 ± 0.02
Overall efficiency for $E_{vis} \geq 140$ PE	0.34 ± 0.04
Additional cuts for $E_{vis} < 140$ PE:	
no cosmic muon in 51.2 μs prior to e^-	0.88 ± 0.01
particle identification on electron[a]	0.86 ± 0.03
Overall efficiency for $E_{vis} < 140$ PE	0.25 ± 0.03

[a]Efficiency for electron identification was determined using the electrons from the decay of muons produced in the higher energy quasielastic events.

signal is in this lowest energy region.) A total of 270 events pass these selection criteria.

In this sample, the most important beam-related background is from π^- DIF followed by $\bar{\nu}_\mu + p \rightarrow \mu^+ + n$. This process was calculated (using the cross section and form factors in Ref. [10]) to give 14 ± 5 events. Contributions from the two other neutrino-related backgrounds, $\bar{\nu}_\mu + {}^{12}C \rightarrow \mu^+ + X$, and $\nu_\mu + {}^{13}C \rightarrow \mu^- + X$, are closely related to the cross section being measured, and were estimated to be less than 4% of the observed yield. From the number of events recorded with the beam off, we infer that 40 ± 2 of the 270 events are due to the cosmic-ray-induced background that passes the selection criteria. All histograms shown for this sample have this beam-off contribution subtracted on a bin-by-bin basis.

Figure 2(a) shows the spectrum of time differences between the muon and electron candidates in our final sample. This figure implies a mean muon lifetime of 2.1 ± 0.2 μs, consistent with expectation. The spatial separation between the μ and e candidates in each pair is shown in Fig. 2(b). The muons are distributed uniformly throughout the fiducial volume. The energy spectrum of the decay electrons is shown in Fig. 2(c). To demonstrate that this energy spectrum is representative of that produced by the decay of muons in LSND, the (normalized) energy spectrum of electrons from the decay of stopped cosmic muons is also shown.

The charge measured in LSND from $C(\nu_\mu,\mu^-)X$ events comes from both the μ^- and the (usually) ejected proton. The light output as a function of particle energy differs for the semirelativistic muons and nonrelativistic protons. A 180 MeV incident neutrino, for example, produces a quasielastic event with total PMT charge between 400 and 600 PEs, depending on the sharing of available kinetic energy between the final state μ^- and p [3]. Events with summed PMT charge greater than 1500 PEs correspond to neutrino energies above 230 MeV. Because it is not possible to accurately recover the energy of the muon or the incident neutrino given only the total charge detected, we show in Fig. 3 the spectrum of collected charge for the quasielastic events, measured in terms of PEs. The collected charge spectrum predicted by a Coulomb-corrected Fermi-gas model (FGM) [1], normalized to the total number of observed events, is superimposed on the data in Fig. 3. For additional comparison, the calculated [10] charge spectrum of ν_μ on free neutrons, also normalized to the data, is shown in the same figure. (These calculated spectra have a systematic uncertainty in their charge scales, arising mostly from uncertainty in the amount of light produced by highly ionizing low-energy protons. For 180 MeV neutrinos, the scale uncertainty in the calculated spectra of collected charge is $\pm 20\%$; the effect of any such rescaling factor increases at lower energies.) The shapes of both calculated spectra agree with the shape of the experimental data. A similar level of agreement was also obtained with a low statistics sample of quasielastic events reported by the E645 Collaboration at LAMPF [11]. The general agreement between the data and both the free neutron and FGM calculations in Fig. 3 indicates that the spectrum shape is not particularly sensitive to the nuclear dynamics which these models do not include.

The cross section for the exclusive reaction $^{12}C(\nu_\mu,\mu^-)^{12}N(\text{g.s.})$ to the ground state can be predicted

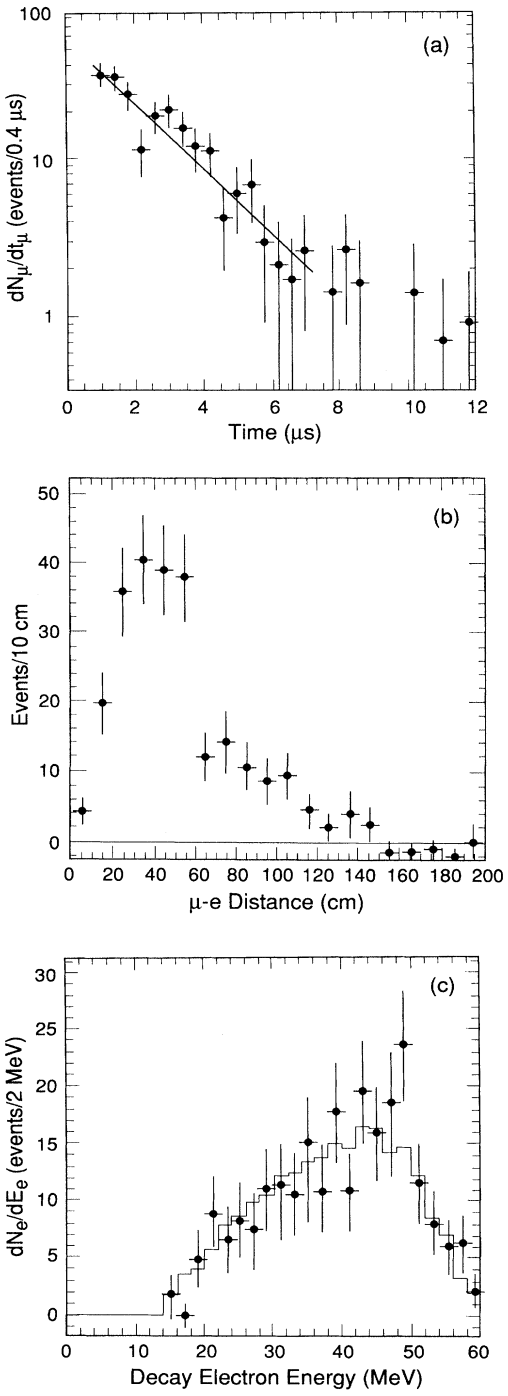

FIG. 2. (a) Time difference between muon and electron candidates. An exponential fit yields a lifetime of 2.1 ± 0.2 μs. Muons that live less than 0.7 μs do not appear in the sample because of the time required for the trigger to reset. (b) Distance between the reconstructed positions of the muon and electron in quasielastic events. (c) Energy of the electron from muon decay. Data points show the electron energy spectrum from the decay of quasielastically produced muons. The histogram shows the spectrum obtained from a sample of stopping cosmic muons. Data points have beam-off contributions subtracted bin-by-bin in all three plots.

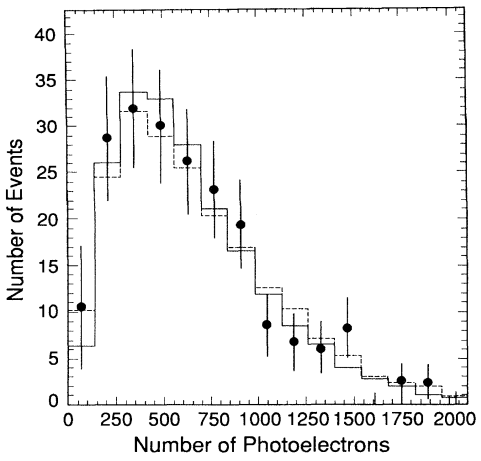

FIG. 3. Data points with error bars show the detected charge distribution of quasielastic events ($\bar{\nu}_\mu p$ and beam-off contributions subtracted bin-by-bin) compared with that predicted by the Fermi-gas model [1] scaled to the data (solid line), and the predicted spectrum from scattering on free neutrons [9], scaled to the data (dashed line). The lowest energy events correspond to neutrinos at the threshold for $C(\nu_\mu,\mu^-)X$; the highest, to neutrinos of 250 MeV and greater.

with certainty as it depends only on form factors measured in beta decay, muon capture, and electron scattering involving the same initial and final states. Fortuitously, this yield can be measured because the ^{12}N ground state is the only ^{12}N level stable against strong decay, so its subsequent beta decay ($E_0=16.3$ MeV, $\tau=15.9$ ms) is a unique and accessible signature. Using the predicted cross section [12] with our calculated neutrino fluxes and detection efficiencies, we would expect to observe seven such events in this data sample. We observe six, giving us some increased confidence in the fluxes and efficiencies employed.

The net number of *inclusive* $^{12}C(\nu_\mu,\mu^-)X$ events detected (after subtracting the beam-off and three beam-related backgrounds) is 210 ± 17 events. This corresponds to a flux-averaged inclusive cross section of $[8.3\pm0.7(\text{stat})\pm1.6(\text{syst})]\times10^{-40}$ cm^2 in the energy region $123.7<E_\nu<280$ MeV. The flux-weighted average neutrino energy is $\langle E_\nu\rangle=180$ MeV. This average cross section is lower than that obtained using the FGM (24×10^{-40} cm^2) and a recent continuum random-phase approximation (RPA) calculation [12] (20×10^{-40} cm^2) evaluated with the flux shown in Fig. 1. An earlier estimation [13] using the measured μ^- capture rates on ^{12}C in conjunction with a closure approximation produces a flux-averaged cross section of 11×10^{-40} cm^2, in agreement with our measurement. However, it is not clear that this method can be reliably extrapolated to the present case as there are no contributions from $l\geq2$ present in the capture rate. These higher partial waves are expected to contribute about half the total yield in the present case.

Our measurement is substantially lower than the average cross section reported by an earlier experiment [14] involving a brief exposure of a less massive, segmented detector to a different (and slightly higher energy) neutrino beam at LAMPF. This previous measurement reported a visible energy spectrum significantly softer than that predicted by the FGM.

We can also compare our results with two earlier measurements [15,16] of $^{12}C(\nu_e,e^-)X$ where the ν_e originate from muon DAR, and therefore are substantially lower in energy than the neutrinos employed in our study. The two measurements of the cross section to the ground state of ^{12}N agree within 15% and with the expected value. (As mentioned earlier, the cross section to the ground state can be fixed using empirically determined form factors.) The measurements of the cross section to excited states of ^{12}N $\{(3.6\pm2.7)\times10^{-42}$ cm^2 [15] and $(6.4\pm2.0)\times10^{-42}$ cm^2 [16]$\}$ span a factor of 2, but within their quoted errors are not in disagreement. Predictions for this inclusive cross section are less well founded than for the ground state transition and also span a factor of 2 $\{6.3\times10^{-42}$ (RPA), and 3.7×10^{-42} [17]$\}$.

Thus there appears to be agreement at the level of about a factor 2 between measurement and calculation for the inclusive cross section to excited states of ^{12}N for low-energy neutrinos on ^{12}C. The ratio of our measured cross section to that predicted using an RPA calculation [12] is 0.42 ± 0.09. It will be interesting to reconcile this result with a yield as large as that reported by Ref. [16] for the lower energy ν_e, as they find a ratio of 1.02 ± 0.32 relative to an RPA calculation. LSND will obtain higher statistics data on both processes in the future and should be able to resolve the experimental situation.

The authors gratefully acknowledge the technical contributions of V. Armijo, K. Arndt, D. Callahan, B. Daniel, S. Delay, C. Espinoza, C. Gregory, D. Hale, G. Hart, E. Khosravi, W. Marterer, and T. N. Thompson to the construction and operation of LSND. We also want to thank the students G. Anderson, C. Ausbrooks, B. Bisbee, T. Chang, L. Christofek, M. Davis, D. Evans, J. George, S. Gomulka, B. Homann, R. Knoesel, S. Lueder, S. Mau, T. Phan, F. Schaefer, M. Strickland, M. Volta, S. Weaver, and K. Yaman for their help in making the detector operational. This work was supported by the U.S. Department of Energy and by the National Science Foundation.

[1] T. K. Gaisser and J. S. O'Connell, Phys. Rev. D **34**, 822 (1986); W. M. MacDonald, E. T. Dressler, and J. S. O'Connell, Phys. Rev. C **19**, 455 (1979). The ^{12}C nucleus is modeled with binding energy 25 MeV, Fermi momentum 220 MeV/c, and 6 neutrons.

[2] Ch. Berger *et al.*, Phys. Lett. B **227**, 489 (1989); R. Becker-Szendy *et al.*, Phys. Rev. D **46**, 3720 (1992); K. S. Hirata *et al.*, Phys. Lett. B **280**, 146 (1992); M. Goodman, in Proceedings of Neutrino '94 [Supplements to Nucl. Phys. B (to be published)].

[3] R. A. Reeder *et al.*, Nucl. Instrum. Methods Phys. Res. Sect. A **334**, 353 (1993).

[4] K. McIlhany, D. Whitehouse, A. M. Eisner, Y-X. Wang, and D. Smith, in Proceedings of the Conference on Computing in High Energy Physics, 1994 (in press).
[5] J. Napolitano *et al.*, Nucl. Instrum. Methods Phys. Res. Sect. A **274**, 152 (1989).
[6] R. L. Burman, M. E. Potter, and E. S. Smith, Nucl. Instrum. Methods Phys. Res. Sect. A **291**, 621 (1990).
[7] R. C. Allen, H. H. Chen, M. E. Potter, R. L. Burman, J. B. Donahue, D. A. Krakauer, R. L. Talaga, E. S. Smith, and A. C. Dodd, Nucl. Instrum. Methods Phys. Res. Sect. A **284**, 347 (1989).
[8] R. C. Allen *et al.*, Phys. Rev. D **47**, 11 (1993).
[9] T. Suzuki, D. F. Measday, and J. P. Roalsvig, Phys. Rev. C **35**, 2212 (1987).
[10] C. H. Llewellyn Smith, Phys. Rep. **3**, 262 (1972); E. J. Beise and R. D. McKeown, Comments Nucl. Part. Phys. **20**, 105 (1991).
[11] S. J. Freedman *et al.*, Phys. Rev. D **47**, 811 (1993).
[12] E. Kolbe, K. Langanke, and S. Krewald, Phys. Rev. C **49**, 1122 (1994); K. Langanke, private communication.
[13] C. W. Kim and S. L. Mintz, Phys. Rev. C **31**, 274 (1985).
[14] D. D. Koetke *et al.*, Phys. Rev. C **46**, 2554 (1992); see also B. Cortez *et al.*, in *Proceedings of the 1981 Orbis Scientiae, Gauge Theories, Massive Neutrinos, and Proton Decay*, edited by A. Perlmutter (Plenum, New York, 1981).
[15] R. C. Allen *et al.*, Phys. Rev. Lett. **64**, 1871 (1990); D. A. Krakauer *et al.*, Phys. Rev. C **45**, 2450 (1992).
[16] B. Zeitnitz *et al.*, Prog. Part. Nucl. Phys. **32**, 351 (1994).
[17] T. W. Donnelly, Phys. Lett. **43B**, 93 (1973); private communication.